Generation of Combined-Modality Tetrahedral Meshes

Karli Gillette[1], Jess Tate[1], Brianna Kindall[1], Peter Van Dam[2], Eugene Kholmovski[1], Rob S. MacLeod[1]

[1] University of Utah, Salt Lake City, Utah, United States of America
[2] Radbound University Medical Center, Nijmegen, Netherlands

Abstract

Registering and combining anatomical components from different image modalities, like MRI and CT that have different tissue contrast, could result in patient-specific models that more closely represent anatomical structures than a model based on either modality alone. In this study, we combined a pair of CT and MRI scans of a pig thorax from two different subjects to make a tetrahedral mesh. Registration of the images is a challenging step in any multimodal imaging and we compared four different registration techniques including rigid, affine, thin plate spline morphing (TPSM), and iterative closest point (ICP), to superimpose the segmented bones from the CT scan on the soft tissues segmented from the MRI. We achieved best visual results with TPSM and affine techniques, which both resulted in the bones remaining close to, but not overlapping, important soft tissue. We also compared simulated results from computing ECGs and defibrillation potentials based on the original MRI model and combined geometric models of the torso. Both qualitatively and quantitatively, the combined geometric models performed similarly to the original MRI model.

1. Introduction

Generating image based models for simulation can be difficult due to limitations of different image modalities. Each modality has strengths and weaknesses for different tissue types. For example, magnetic resonance imaging (MRI) has high soft tissue contrast but lacks bone contrast to robustly segment bones. X-ray computed tomography (CT), by comparison, has high bone contrast, but the heart, lungs, and blood volume are poorly resolved.

Creating models from both MRI and CT, has the advantage of leveraging the strengths of both to achieve higher accuracy than from either modality alone. Such improvements are especially valuable for bioelectric field simulations in which soft tissue and regions of bone are in close proximity. Previous dual modality examples include modeling of transcranial electrical and magnetic stimulation in the brain[1] and we anticipate similar improvements in cardiac bioelectricity applied to ECG Imaging [2] and to simulation of defibrillation [3,4].

In this study, we addressed a particularly challenging problem of aligning images from MRI and CT scans from different subjects. We created mutli-modality, tetrahedral meshes for cardiac bioelectricity simulations by registering the bone geometry from a CT scan of one pig with the MRI segmentation of a second. Techniques included thin plate spline morphing (TPSM), affine, rigid, and iterative closest point (ICP) [5] registration and the results were compared to the segmentation from the MRI. In order to evaluate the impact of the registration errors from this dual-modality, dual-subject approach, we then compared ECG and cardiac defibrillation simulation results between the combined model and one derived only from MRI.

2. Methods

Figure 1 shows the pipeline for developing the multi-modality, tetrahedral meshes using the open source software from the Center for Integrate Biomedical Computing (www.sci.utah.edu/cibc).

Two adult pigs were scanned, one with MRI and the other with CT and the images were segmented separately into different tissue types using Seg3D [6]. Using Cleaver2 [7], we then created tetrahedral meshes that included the tissue regions associated with the torso, heart, lungs, blood, and bones.

For image based registration, we identified a total of 70 correspondence points throughout the entire geometry, but mainly focused on the ribcage, sternum, heart and other stationary locations within the torso. A subset of 37 points, selected using the Ransac algorithm [8] that identifies outliers in data given a certain fitting technique (rigid, affine, etc.), was used to perform affine, rigid, and TPSM registration techniques. We applied an additional registration approach, known as ICP [5], to align the geometries based on the meshes from the two image sets.

The results of the different registration techniques were evaluated quantitively using the DICE coefficient [9],

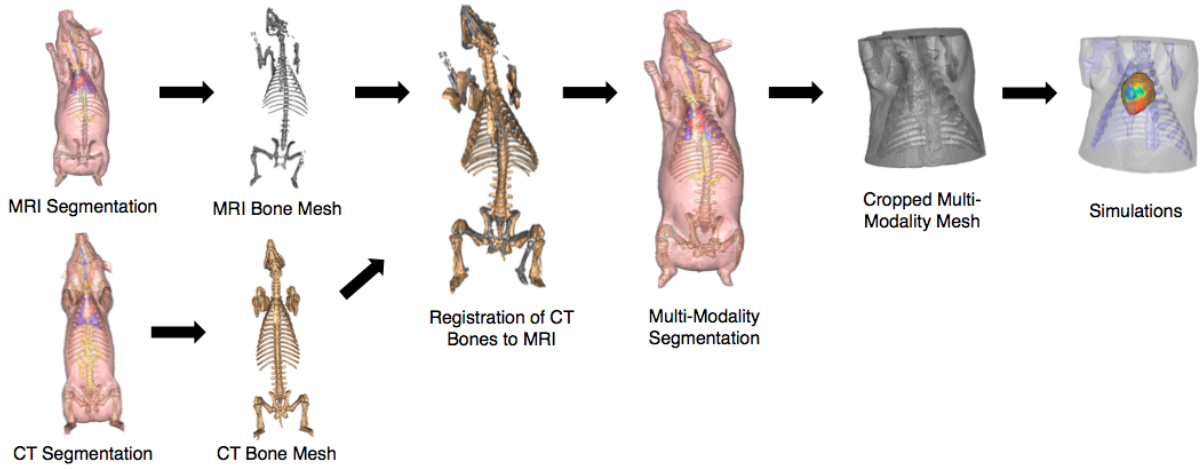

Figure 1: A general pipeline for generating combined image-based tetrahedral meshes for simulation.

Hausdorff distance [10] and RMS error metrics. All registrations and metric computations were performed using custom programs written in MATLAB (The MathWorks, Inc.), except for Affine and TPSM, which were implemented in SCIRun[11].

We generated multi-modality models using the methods that performed the best in terms of the image-based metrics: affine and TPSM. During this process, implemented within Seg3D, the MRI bones were added to the torso layer in the MRI segmentation. The registered CT bones segmentation was removed from the MRI torso layer and overlap between all layers removed. The MRI thorax segmentations now contained the registered CT bone segmentation instead of the original MRI bones. Tetrahedral meshes were created from the cropped, combined-modality segmentations using Cleaver2.

In order to evaluate the impact of errors in geometric alignment between the two modalities on our target applications, we carried out simulations of the ECG and internal cardiac defibrillation (ICD) using the generated affine multi-modality, TPSM multi-modality, and, to serve as the baseline, the original MRI mesh. To isolate the effects of bone we carried out each simulations again with the bone conductivity set to the torso conductivity. The source of heart potentials for the ECG model [12] were recorded epicardial potentials from a canine heart mapped onto the MRI based model of the heart surface. We then computed the associated body-surface ECGs using the Forward/Inverse Toolbox in SCIRun [12]. The ICD simulations followed a standard procedure [3] of placing electrodes within each model using modular software within SCIRun. Defibrillation thresholds and the torso potential distribution were then calculated. Error metrics included percent error, correlation coefficient, and RMS error.

3. Results

Quantitative error metrics for registration are displayed in Table 1. Comparatively, the TPSM-registered bones have the smallest tissue overlap, highest bone overlap, highest Dice coefficient, and a lower RMS error. Though rigid registration exhibited the lowest Hausdorff distance, the method also had the highest tissue overlap and lowest bone overlap. Both ICP and affine registration quantitatively performed similarly, though affine had a higher Dice coefficient and higher bone overlap while ICP had a lower RMS error and tissue overlap.

Table 1: Error metrics for different registration techniques.

Error Metric	TPSM	Affine	Rigid	ICP
Dice Coefficient	0.23	0.11	0.07	0.10
Hausdorff Distance (mm)	165	172	118	150
RMS Error (mm)	25.3	32.8	31.8	23.8

Qualitative comparison indicated that both TPSM (Figure 2a) and affine (Figure 2b) align the general spinal, sternum and ribcage curvatures well. Bones from both methods remained close to, but not overlapping, soft tissue of the heart, lungs, and blood volume. Both the rigid (Figure 2c) and ICP (Figure 2d) registration showed noticeable deviation from the MRI bones, especially along the spine, leading to overlap with the heart and lungs. All methods resulted in noticeable deviation of the head and legs.

Both multi-modality meshes, with or without bones, produced similar results to the original MRI mesh in the ICD (Figure 3) and ECG simulations (Figure 4). However, the boneless MRI preformed most comparably to the original MRI in both simulations. The ICD simulations

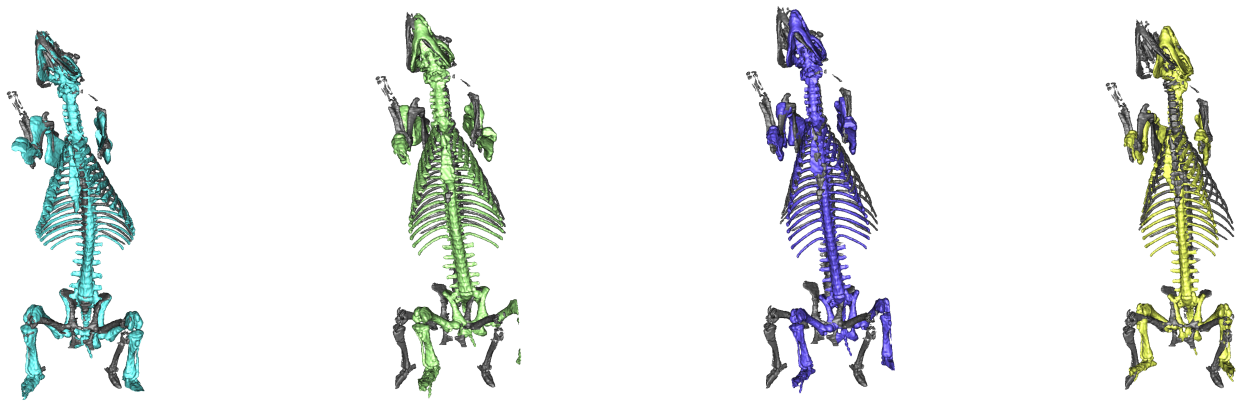

(a) TPSM (b) Affine (c) Rigid (d) ICP

Figure 2: CT Bones registered usingTPSM, rigid, affine, and ICP techniques compared to the original MRI Bones.

yielded defibrillation thresholds of 8.1 J, 8.2 J, and 9.7 J for the original MRI, affine mutli-modality, and TPSM mutli-modality mesh, respectively. Error metrics for the ICD simulation are shown in Table 2 and the ECG simulations in Table 3.

4. Discussion

The tetrahedral meshes generated using both TPSM and affine registration techniques were of high enough quality to use in simulated applications that compared in performance to the original MRI Mesh (Figures 3 and 4). Other registration techniques may also be effective for generating multi-modality meshes given minimal soft tissue overlap in the region of the heart and lungs. Preliminary data suggests (not shown here) that performing registration on cropped meshes that neglect the legs and head, may lead to better error metrics and less soft tissue overlap around the domain of the heart. Additionally, registration techniques could be used sequentially. For example, TPSM could be followed by ICP to get further refinement of the registered CT Bones.

Table 2: Error metrics for ICD Simulation:

Method	Correlation Coefficient	Percent Error (%)	RMS Error (V)
with bones:			
TPSM	0.98	4.5	57
Affine	0.98	3.9	53
without bones:			
MRI	1.0	0.018	3.5
TPSM	0.98	4.4	56
Affine	0.98	3.8	52

Table 3: Error metrics for ECG Simulation

Method	Correlation Coefficient	Percent Error (%)	RMS Error (mV)
with bones:			
TPSM	1.00	0.22	0.05
Affine	1.00	0.23	0.05
without bones:			
MRI	1.00	0.13	0.04
TPSM	1.00	0.26	0.05
Affine	1.00	0.25	0.05

Our preliminary results suggest that the impact of including realistic bone geometry on simulation results was minimal, which suggests that including bones in a torso model may not yield significant improvements. However, more extensive comparison will be necessary to evaluate this initial finding, including further evaluation of mesh quality and interpolation errors that may impact simulation results.

In general, taking advantage of the strengths of each modality by generating mutli-modality meshes is feasible. The pipeline we developed can generate torso geometries from a variety of modalities possibly even using different specimens. This finding suggests that patient specific models could be created using an arbitrary CT scan of an alternative patient, thus limiting radiation exposure and possibly improving clinical impact.

Acknowledgements

This project was supported by the National Institute of General Medical Sciences of the NIH under grant P41 GM103545-17.

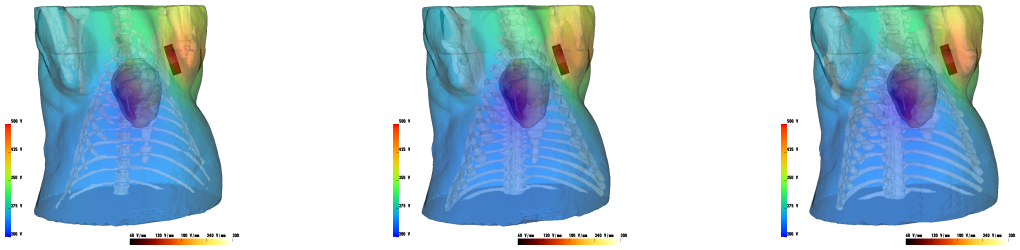

Original MRI TPSM Affine

Figure 3: ICD defibrillation discharge potentials of the original torso mesh (first) compared to the TPSM composite mesh (second) and affine composite mesh (third) given the same ICD placement and an initial 500 V shock.

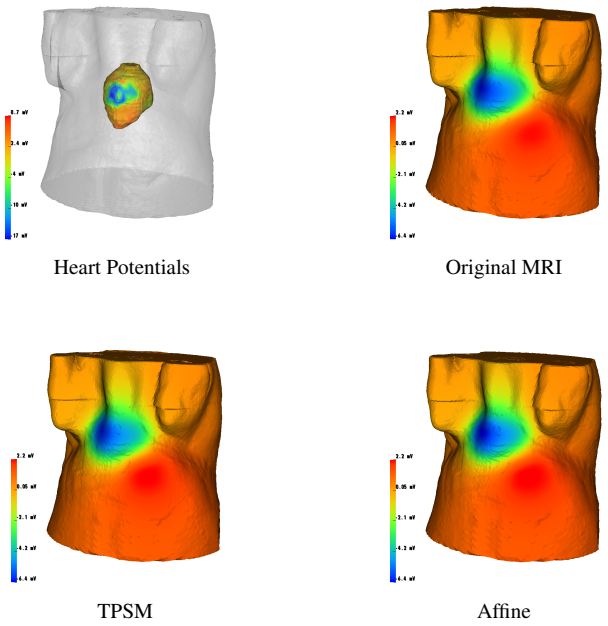

Heart Potentials Original MRI

TPSM Affine

Figure 4: ECG Forward simulations show heart surface potentials (top left) and corresponding surface potential estimation on the original MRI mesh (top right), TPSM composite mesh (bottom left), and affine composite mesh (bottom right).

References

[1] Dannhauer M, Brooks D, Tucker D, MacLeod R. A pipeline for the simulation of transcranial direct current stimulation for realistic human head models using SCIRun/BioMesh3D. Proceedings of the IEEE Engineering in Medicine and Biology Society 34th Annual International Conference Aug 2012;2012:5486–5489.

[2] Rudy Y, Lindsay B. Electrocardiographic imaging of heart rhythm disorders: from bench to bedside. Card Electrophysiol Clin Mar 2015;7(1):17–35.

[3] Jolley M, Stinstra J, Tate J, Pieper S, MacLeod R, Chu L, Wang P, Triedman J. Finite element modeling of subcutaneous implantable defibrillator electrodes in an adult torso. Heart Rhythm J May 2010;7(5):692–698.

[4] Tate J, Pilcher T, Aras K, Burton B, MacLeod R. Verification of a defibrillation simulation using internal electric fields in a human shaped phantom. In Computing in Cardiology Conference (CinC), 2014, volume 41. 2014; 689–692.

[5] Besl P, McKay N. A method for registration of 3-D shapes. IEEE Trans Pat Anal Mach Intellig 1992;14(2):239–256.

[6] CIBC, 2015. Seg3D: Volumetric Image Segmentation and Visualization. Scientific Computing and Imaging Institute (SCI), Download from: http://www.seg3d.org.

[7] CIBC, 2015. Cleaver: A MultiMaterial Tetrahedral Meshing Library and Application. Scientific Computing and Imaging Institute (SCI), Download from: http://www.sci.utah.edu/cibc/software.html.

[8] Fischler MA, Bolles RC. Random sample consensus: A paradigm for model fitting with applications to image analysis and automated cartography. Communications of the ACM 1981;24:381–395.

[9] Dice LR. Measures of the amount of ecologic association between species. Ecology 1945;27:297–302.

[10] Huttenlocher DP, Klanderman GA, Rucklidge WJ. Comparing images using the hausdorff distance. IEEE Trans Pat Anal Mach Intellig 1993;15:850–863.

[11] Institute S, 2015. SCIRun: A Scientific Computing Problem Solving Environment, Scientific Computing and Imaging Institute (SCI), Download from: http://www.scirun.org.

[12] Burton B, Tate J, Erem B, Swenson D, Wang D, Brooks D, van Dam P, MacLeod. R. A toolkit for forward/inverse problems in electrocardiography within the scirun problem solving environment. In Proceedings of the IEEE Engineering in Medicine and Biology Society 33rd Annual International Conference. 2011; .

Address for correspondence:

Karli Gillette
University of Utah, 72 Central Campus Dr, Salt Lake City, UT, USA 84112
karli.gillette@utah.edu